A Finite State Machine Model to Represent Inverters in Photovoltaic System Simulations

Anton Driesse*, Steve Harrison†, and Praveen Jain*
*Dept. of Electrical Engineering
†Dept. of Mechanical Engineering
Queen's University, Kingston, Canada
Email: driessea@queensu.ca

***Abstract*—The simulation of Photovoltaic (PV) Power Systems relies on appropriate models of the PV array, power conversion electronics, operating conditions and sometimes, energy storage and loads. This paper presents a model of intermediate complexity for grid-tie inverters that can capture many differences between specific products, yet remains generic enough to be used without expert knowledge of their internal circuits. The core of this model is a *finite state machine* (FSM) that defines the typical operating modes, or states, of grid-tie inverters and the conditions that lead to transitions from one state to another. Each state also defines parameters related to the transfer of electrical power, such as operating limits, conversion losses and maximum power point tracking efficiency. The increase in inverter temperature resulting from electrical losses is also modeled.**

Introduction

Power conversion equipment such as grid-tie inverters are key components in photovoltaic power systems. They may represent only a fraction of the system cost, and do not even appear in most system photographs, but they influence system performance to a large extent. A seemingly small improvement in efficiency, for example, reduces the number of PV modules needed for a given energy output, and can therefore reduce total system cost significantly.

Although their basic function is simple, inverters are usually complex devices. Much of that complexity stems from the control systems that are needed to track the maximum power point, detect and respond to islanding conditions, ensure the operation stays within safe boundaries (e.g. temperature, voltage), and perhaps perform self-diagnostics. All these functions are in addition to the fundamental control for the switching elements to produce a clean sinusoidal output current and voltage.

Research activities often focus on one or two aspects of the inverter, and the models that are developed in the process are not usually appropriate for full system simulations. Time-steps are typically in the order of milliseconds or microseconds, which is neither necessary nor practical to evaluate long-term energy yields; nor is it appropriate for integration with other simulation domains, for example, to analyze more complex building-integrated systems. At the other end of the spectrum, in system-level models for design or simulation the inverter is often represented very simply as an ideal component, or one with a fixed percentage loss.

The present effort is motivated by the need to simulate PV systems that are tightly integrated into solar buildings: buildings that make use of multiple solar energy technologies to target net zero consumption. In such buildings PV performance is not necessarily optimized, but rather overall building performance is optimized. This can lead to non-typical operating conditions for the PV array, such as higher cell temperatures or partial shading. More importantly, such buildings will deploy advanced control strategies for both thermal and electrical systems that can alter the operating conditions much faster than would naturally occur in static designs. For example, air circulation beneath a PV array may be stopped or started using blowers and dampers. As a result, PV system component models used in this context must be accurate on a much shorter time scale than in general. However, advances made in improving the accuracy and resolution of the models for this purpose may of course be applied to all contexts.

Model Design

The principal objective of the model is to determine how much power—and over time, energy—is transferred from the PV array to the utility grid. Real inverters never transfer the maximum available power from a array into the grid. There are three reasons for this: some power is lost in the power inversion stage, some power is inadvertently not extracted from the array due to maximum power point tracking (MPPT) error, and some power is purposely not extracted because of a control decision. Furthermore, there are times when power is taken out of the grid, rather than fed into it. The proposed model captures all of these aspects.

The target simulation time step for our simulations is in the order of one second to one minute. At this time resolution all the important interactions with thermal domain and control systems are expected to be captured

978-1-4244-1668-4/08/$25.00

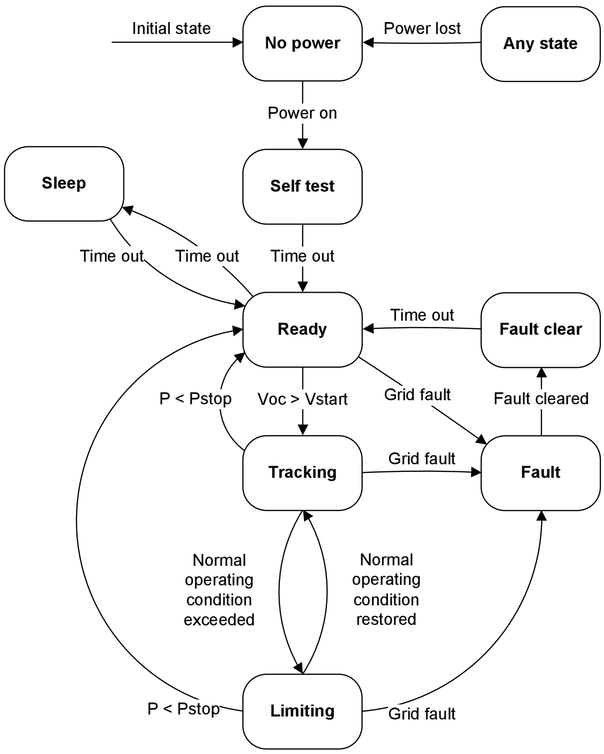

Fig. 1. Finite State Machine to control a grid-connect inverter

adequately. Thermal masses limit temperature changes during such a short time, and controls incorporate delays or hysteresis to limit the frequency of transitions. And while solar irradiance can vary significantly during one minute, or sometimes even during one second, assuming a constant value over such a short time step is deemed adequate for the solar building context.

The Finite State Machine

Control decisions made within the inverter are represented by a finite state machine (FSM). The states and transitions are chosen to be generic enough to represent all inverters, and individual inverters are simulated by adjusting various parameter values. The diagram in Fig. 1 shows the states, transitions, and several of the parameters affecting the control decisions. Although there are many parameters, most are usually documented in the inverter manual.

Most of the transitions occur as a result of conditions detected inside the inverter, such as time-out delays and various operating constraints, whereas others occur as the result of explicit external signals such as a grid-fault indicator. Islanding or grid fault detection itself is not possible with this type of model, but simulating system response to an islanding condition is.

The following paragraphs describe the states that appear in Fig. 1 and the conditions that lead to transitions. The most important parameters are also summarized in Table I.

No power: This is the initial condition. No power is produced or consumed by the inverter. A logic signal indicates when grid power is available, and causes a transition from any other state to the *Power off* state when power is lost.

Self test: This state is merely a delay before the inverter can begin to operate. In real inverters this delay may be a combination of things including self diagnostics - which the model assumes will succeed. The inverter consumes some power from the grid at this stage.

Ready: The inverter is not active, but is monitoring the array conditions to see whether it should start. The main start condition is sufficient array voltage, V_{start}. This must be maintained for some time in order to avoid false starts. Power consumption in this state is usually low.

Sleep: Some inverters advertise an even lower power consumption during the night. Although, we have found no clear descriptions of how they switch between *Ready* and *Sleep* modes, it could certainly be done based on the real-time clock that most inverters have now, or by sensing V_{oc}.

Tracking: Once the array provides sufficient stable voltage, the inverter begins to convert the available DC power to AC. The nominal operating point is V_{mpp}. The losses are calculated as a function of power and input voltage, and converted to heat. This heat causes the internal inverter temperature to increase and dissipates into the surrounding space which may be at room temperature or exterior air temperature depending on the installation. When integrated into a whole-building simulation, this will contribute to the internal gains. Tracking will stop and the inverter will return to *Ready* mode if the power

TABLE I
KEY PARAMETERS CONTROLLING THE INVERTER STATE

Parameter	Description
$T_{selftest}$	Amount of time after power-up before reaching the *Ready* state.
V_{start}	Open circuit voltage threshold to enter the *Tracking* state.
T_{start}	Duration open circuit voltage must remain above V_{start} before making a transition. The voltage must also remain below V_{max}.
P_{stop}	Output power level threshold to stop tracking and return to the *Ready* state.
T_{stop}	Duration the output power must remain below P_{stop} before making a transition.
P_{max}	Maximum input power of the inverter, beyond which limiting (or a fault) occurs.
I_{max}	Maximum input current of the inverter, beyond which limiting (or a fault) occurs.
T_{max}	Maximum temperature inside the inverter, beyond which limiting (or a fault) occurs.
V_{mpp_min}	Minimum input voltage of the inverter, beyond which limiting (or a fault) occurs.

remains below a threshold, P_{stop}.

Limiting: Various conditions may cause the inverter to reduce its output power from the maximum, such as excessive current, excessive power, or excessive temperature, or insufficient array voltage. In all cases the operating voltage is increased to keep these values within the proper range. Some inverters may shut down completely for a brief period of time under some or all of these conditions instead of implementing this limiting behaviour. This would result in a transition to the *Fault* state.

Fault: The fault state can also be reached by a logic signal that indicates a grid fault. Such a condition can not be detected in this system model, but can be imposed to illustrate the effect on the system (the inverter cools off and the array heats up).

Fault clear: After the fault is cleared a delay is usually imposed before a resumption of normal operation in order to reduce the likelihood of the inverter re-entering the fault state immediately.

The main parameters governing the transitions between states are summarized in Table I

Interaction with the PV Array Model

In the *Tracking* and *Limiting* states the inverter must interact with the PV array to establish the DC operating point. For the purpose of demonstrating the inverter model a well-known PV cell/array model was used: the single-diode model with both shunt and series resistances which is described in many sources, such as [1]. Temperature dependencies of the model parameters were taken from the same source and the method to calculate the cell temperature is based on [2]. These equations are used to determine, V_{oc} and V_{mpp} under any set operating conditions, as well as current and power for any given array voltage.

The flow chart in Fig. 2 illustrates how the different components of the inverter model interact with the PV array model. As the simulation process is an iterative one, the inverter operation is determined by the current state, and the state for the next iteration is chosen based on the output of the current iteration.

Operating Point Control

The aspect of DC operating point control that usually receives the most attention is maximum power point tracking (MPPT). Maximum power point tracking is represented within this model primarily for the purpose of quantifying the losses that are incurred by imperfect tracking. The simplest way to do this to specify a single parameter η_{mppt} so that $P_{loss,mppt} = P_{mpp}(1-\eta_{mppt})$. Since the PV array model provides P_{mpp} this is easy to implement.

However, if there is an MPPT error, that means the array voltage is not at V_{mpp}. Determining the appropriate array operating voltage that gives rise to this loss is not so

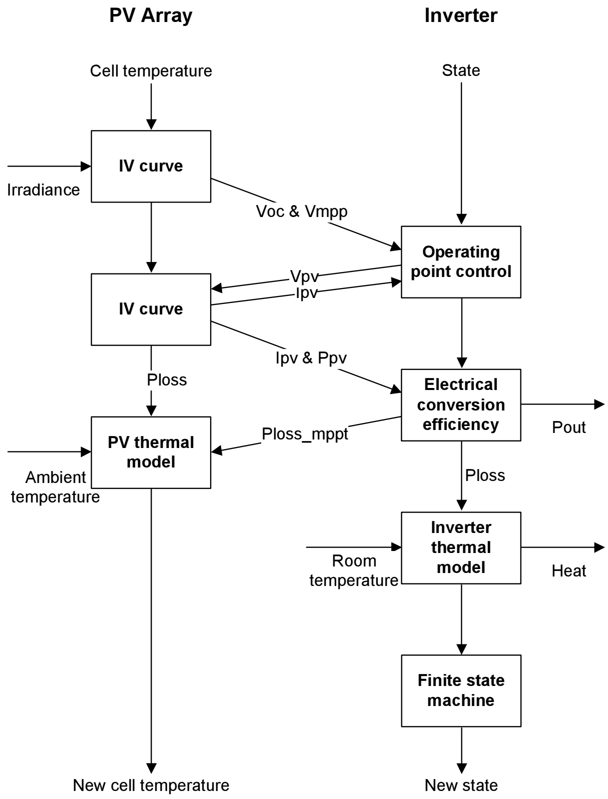

Fig. 2. Flow chart illustrating the principal interactions between the PV array and inverter model components.

simple, since it may fluctuate around the ideal or remain consistently above or below it. We avoid this question by assuming the array *does* operate at V_{mpp}, producing P_{mpp}, but we send $P_{loss,mppt}$ back from the inverter to the array to be dissipated as heat and to maintain the correct energy balance.

The loss described here represents only the steady-state tracking error. A companion parameter $\eta_{mppt,dyn}$ has been proposed recently to provide a basis of comparison between inverters, and is derived from a specific pattern of varying array output power levels [3]. Even if known, however, it is unclear how this parameter would be used to predict $P_{loss,mppt}$ for arbitrary dynamics in array output.

An alternate approach to representing MPPT in the inverter would be to execute the MPPT algorithm within the model. Some methods are trivial to implement, such as setting the operating voltage to a fraction of V_{oc}, whereas the various search methods would add a bit of complexity. The advantage of this approach is that whenever the array operating voltage is different from V_{mpp} and the array output power is reduced automatically by the array model. The downside is that the details of the MPPT algorithm are rarely known for commercial products. What's more, even under controlled experiments it can be difficult to reproduce the same dynamic MPPT behaviour for the same inverter [3].

The second aspect of operating point control, which is the more important aspect in our model, is keeping the DC voltage, current and power as well as the internal inverter temperature all within the normal range of operation. The most favourable behaviour of an inverter is to increase the operating voltage just enough to keep the power, current and temperature from exceeding their limits. Likewise, the operating voltage must be kept above the lower limit of the MPPT range, or above the minimum DC voltage required to produce the correct peak value of the AC waveform. Our inverter model uses a control loop to achieve these objectives, as illustrated by the information passed in both directions between the *IV curve* block and the *Operating point control* block in the flow chart.

The effects of this control loop on inverter operation can be seen in both Figs. 3 and 4. In the first example it is quite a warm day, and particularly at times of low insolation the array MPPT voltage is well below the minimum value of 330 V. The model enforces this constraint, and some of the available energy is not collected from the array as a result. In the second example the inverter's internal temperature limit T_{max} is reached. In response the inverter shifts the DC operating point to reduce the power level and prevent the temperature from rising further. (The inverter thermal model is discussed in greater detail below.)

Electrical Conversion Efficiency

The conversion efficiency η indicates how much of the input power is transferred to the output. The difference, P_{loss}, is converted to heat inside the inverter. The internal losses can be categorized as resistive losses, proportional to I^2; constant voltage drops and switching losses, proportional to I; and other losses that do not vary with output current. Since the output voltage of the inverter does not vary much, the losses are usually expressed as a quadratic function of power instead of current, such as: $P_{loss} = K_0 + K_1 P_{out} + K_2 P_{out}^2$ [4].

Conversion losses can be analyzed based on the internal details of the inverter (see for example [5]), but we prefer to take the black-box approach here. Manufacturers usually provide an efficiency profile for a range of power levels which can then be used to estimate the constants in an equation such as the one above. Independent laboratories also perform such tests and a large set of such reports is made public by the California Energy Commission [6]. These latest data document how inverter efficiency varies with DC input voltage as well, therefore out loss model includes both power and voltage dependencies. Further detail on this aspect is provided in [7].

Self-consumption can make a significant difference to long-term performance, but the quadratic loss equation does not represent this very well if portions of the inverter are deactivated or powered down. The efficiency function

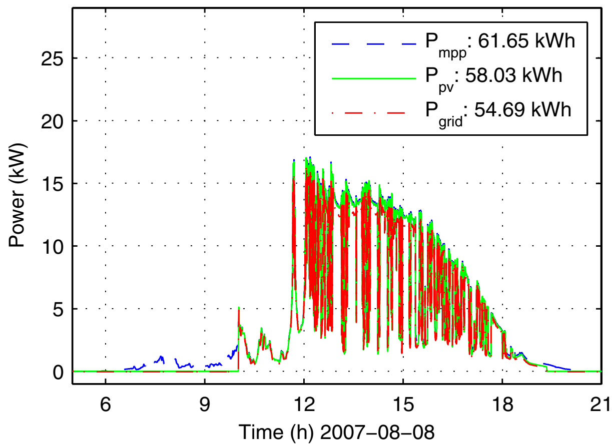

(a) Power levels: MPP, PV output, inverter output.

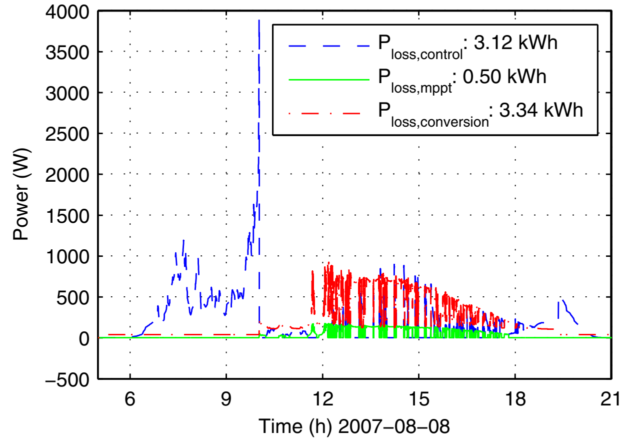

(b) Power losses: control-related, MPP tracking and electrical conversion.

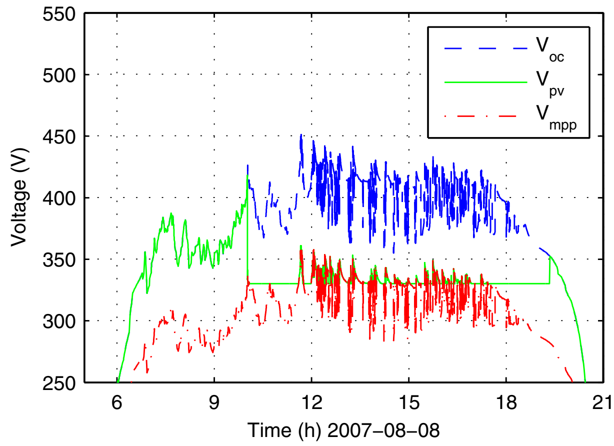

(c) Voltage levels: Open circuit, simulated operating point and MPP.

Fig. 3. Simulations on a partly cloudy day with $V_{start} = 400$. A late start in the day and limiting due to low voltage both contribute to a reduction in daily energy production.

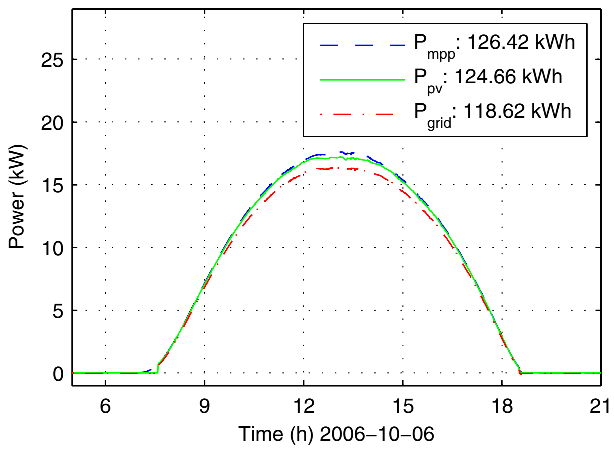

(a) Power levels: MPP, PV output, inverter output.

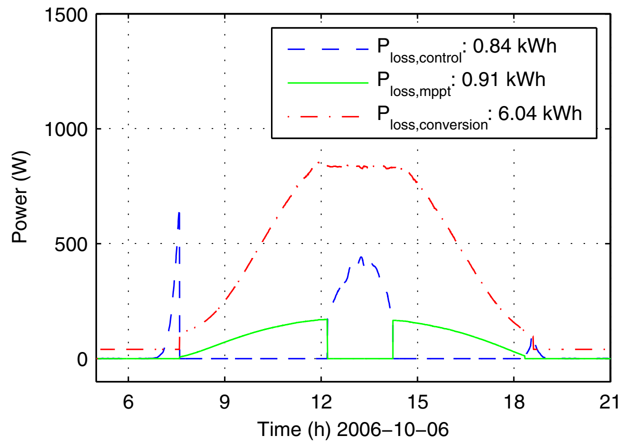

(b) Power losses: control-related, MPP tracking and electrical conversion.

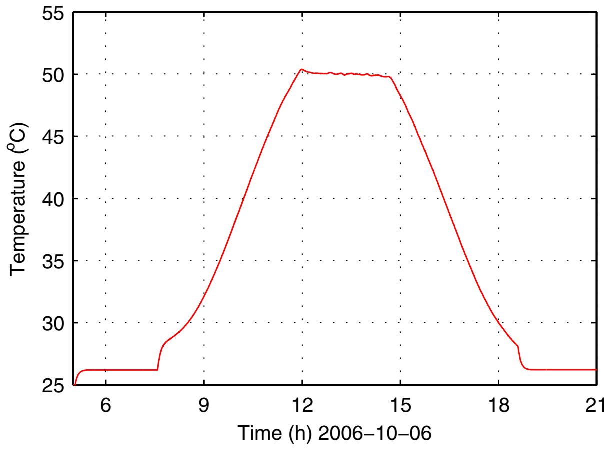

(c) Simulated internal temperature of the inverter.

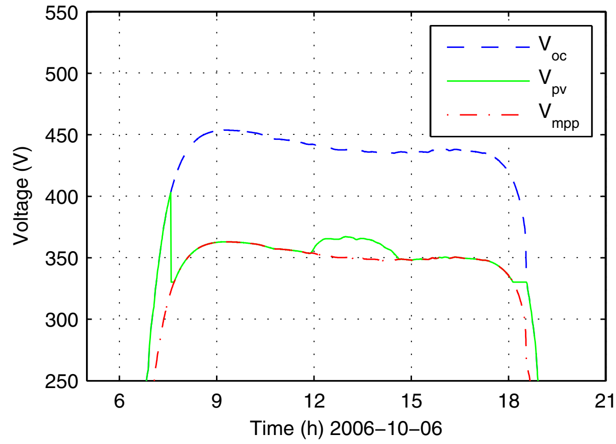

(d) Voltage levels: Open circuit, simulated operating point and MPP.

Fig. 4. Simulations on a clear day with inverter operating at room temperature with $T_{max} = 50$. The inverter limits its output in order to prevent overheating. Throttling or derating behaviour to keep DC current and power within specifications is similar.

then takes various conditionals as in [8]. The advantage of the FSM is that each of these modes or states can have independent loss coefficients, and the best fit for active operation does not need to take into account idle consumption. Furthermore, simulations using the FSM will provide realistic estimates of the *duration* of time spent in each those modes. The overall assessment of system energy yield, whether short- or long-term, should therefore be more accurate.

Inverter Thermal Model

Inverter efficiency affects energy yield, but also the amount of heat generated inside the inverter. High temperatures in an inverter may lead to shut-down, reduction of output power, and/or activation of some cooling enhancer such as a fan. To capture this behaviour in the FSM, the inverter model must include at least a simple thermal model. The thermal model is hard to generalize since cooling is achieved by multiple means (natural and forced convection, radiation, conduction) and the effect of each depends on widely varying physical characteristics of the inverter. Furthermore, the temperature of different components within the inverter will vary significantly.

Despite these complexities, inverters are deemed to have two characteristics in common: heating and cooling are slowed by a thermal mass, and the cooling effect is proportional to the temperature difference between the interior of the inverter and the surrounding air. More precisely stated, if we have a mass of thermal capacity C_T to absorb the electrical losses P_{loss} then we can calculate an internal temperature T_{int} by solving:

$$\frac{dT_{int}}{dt} = \frac{P_{loss} - \dot{Q}}{C_T} \quad (1)$$

The rate of heat loss dissipated to the surroundings, $\dot{Q}$, is estimated using a lumped heat loss coefficient U_L:

$$\dot{Q} = U_L \cdot (T_{int} - T_{amb}) \quad (2)$$

where T_{amb} is the ambient temperature.

The two parameters C_T and U_L are not usually available, but U_L can be estimated from the maximum ambient operating temperature $T_{amb,max}$ under full load as follows:

$$U_L = \frac{P_{loss,max}}{T_{int,max} - T_{amb,max}} \quad (3)$$

where $T_{int,max}$ is the maximum internal temperature. This is not usually available either, but we estimate it to be $80°C$. The parameter C_T is less critical and a value in the order of $10 * P_{out,max}$ produces fairly realistic behaviour.

Fig.4 shows how the model limits power output when the internal inverter temperature exceeds a threshold. In the example the threshold was reduced from the typical $80°C$ to $50°C$ in order to demonstrate this.

Implementation

Both the inverter and the PV array models were implemented in MATLAB using a combination of Simulink building blocks and embedded MATLAB functions. Although the natural way to implement the FSM in MATLAB/Simulink might be to use the Stateflow tool, the simplicity of this particular FSM allowed it to be implemented quite easily in using embedded MATLAB with a `switch` construct and appropriate conditional statements.

In the sample outputs shown, the parameters for both the array and the inverter were taken to represent the PV installation on the Queen's University campus. It consists of 12 strings of 22 modules of type Photowatt PWX750-75 connected to a Xantrex PV-20208 inverter with external isolation transformer. The operating conditions for the model (solar radiation and ambient temperature) were obtained from measurements adjacent to this system.

As designed and built, the array V_{mpp} drops below the specified range of the inverter (330V) on a regular basis, as seen in Fig. 3. However we have observed that our particular inverter does not apply a hard limit as the model does, making the energy estimates of the model somewhat conservative. This seems appropriate from the point of view that systems should not be designed and expected to operate beyond the manufacturers specifications. In the case of the DC operating voltage, too low a value could result in increased distortion in the output waveform - something which is clearly undesirable.

In order to test other forms of limiting behaviour, the relevant parameters were reduced from the specifications because the inverter is generously sized for this array.

Conclusions

Our inverter model incorporating a Finite State Machine provides a very realistic representation of real-world grid-tie inverters. Together with our array model, which is designed to interact with this inverter model, accurate system simulations can be performed. These simulations predict the start-up, shut-down, and limiting behaviour in great detail, and provide a tangible measure of their impact on system energy yields. These detailed results provide extra insight into the trade-offs between different inverter products, and make it possible to achieve the best possible match between array and inverter. Where it is possible to adjust certain inverter control parameters, the model also allows the system designer to perform virtual tests using different values for those parameters.

The inverter electrical efficiency is calculated as a function of both power and voltage, which is described in [7]. The MPPT efficiency is currently specified as a fixed percentage. To reflect the dynamic nature of MPPT, we would like to impose a limit on the rate of change of the operating voltage, however assigning a value to such a parameter to correspond to a specific inverter product is not possible with the information that is typically available.

The next step in the model development will be to implement more complex concepts such as single inverters containing multiple MPPT units or multiple output stages; and multiple inverters working in team or master/slave configuration.

Acknowledgment

The author would like to thank NSERC for the financial support provided to this research project throught the Canadian Solar Buildings Research Network.

References

[1] J. A. Duffie and W. A. Beckman, *Solar Engineering of Thermal Processes*, 3rd ed. Wiley-Interscience, 2006.

[2] O. Ulleberg, "Stand-alone power systems for the future: optimal design, operation & control of solar-hydrogen energy systems," Ph.D. dissertation, Norwegian University of Science and Technology, Trondheim, 1998.

[3] H. Haeberlin, L. Borgna, M. Kaempfer, and U. Zwahlen, "Measurement of dynamic mpp-tracking efficiency at grid-connected inverters," in *21st European Photovoltaic Solar Energy Conference*, Sept 2006.

[4] A. E.-M. M. A. El-Aal, J. Schmid, J. Bard, and P. Caselitz, "Modeling and optimizing the size of the power conditioning unit for photovoltaic systems," *Journal of Solar Energy Engineering, Transactions of the ASME*, vol. 128, no. 1, pp. 40–44, Feb. 2006.

[5] M. Cavalcanti, G. M. S. Azevedo, B. A. Amaral, K. C. de Oliveira, F. A. S. Neves, and D. Lins, "Efficiency evaluation in grid connected photovoltaic energy conversion systems," in *Power Electronics Specialists Conference, 2005. PESC '05. IEEE 36th*, Recife, 2005, pp. 269–275.

[6] California Energy Commision, "Inverter performance test results," http://www.consumerenergycenter.org/erprebate/inverter_tests/index.html, Nov 2007.

[7] A. Driesse, S. Harrison, and P. Jain, "Beyond the curves: Modeling the electrical efficiency of photovoltaic inverters," in *IEEE Photovoltaic Specialists Conference*, San Diego, 2008.

[8] K. Peippo and P. D. Lund, "Optimal sizing of grid-connected PV-systems for different climates and array orientations: A simulation study," *Solar Energy Materials and Solar Cells*, vol. 35, no. 1, pp. 445–451, Sep. 1994.